

A review of elliptic flow of light nuclei in heavy-ion collisions at RHIC and LHC energies

Md. Rihan Haque,^{1,*} Chitrasen Jena,^{2,3,†} and Bedangadas Mohanty^{2,‡}

¹*Utrecht University, P.O. Box 80000, 3508 TA Utrecht, The Netherlands*

²*School of Physical Sciences, National Institute of Science Education and Research, Jatni 752050, India*

³*Indian Institute of Science Education and Research, Tirupati 517507, India*

We present a review of the measurements of elliptic flow (v_2) of light nuclei (d , \bar{d} , t , ${}^3\text{He}$ and ${}^3\bar{\text{He}}$) from the RHIC and LHC experiments. Light (anti-)nuclei v_2 have been compared with that of (anti-)proton. We observed similar trend in light nuclei v_2 as in identified hadron v_2 with respect to the general observations such as p_T dependence, low p_T mass ordering and centrality dependence. We also compared the difference of nuclei and anti-nuclei v_2 with the corresponding difference between v_2 of proton and anti-proton at various collision energies. Qualitatively they depict similar behavior. We also compare the data on light nuclei v_2 to various theoretical models such as blast-wave and coalescence. We then present a prediction of v_2 for ${}^3\text{He}$ and ${}^4\text{He}$ using coalescence and blast-wave models.

I. INTRODUCTION

The main goals of high energy heavy-ion collision experiments have primarily been to study the properties of Quark Gluon Plasma (QGP) and the other phase structures in the QCD phase diagram [1–4]. The energy densities created in these high energy collisions are similar to that found in the universe, microseconds after the Big Bang [2, 5, 6]. Subsequently, the universe cooled down to form nuclei. It is expected that high energy heavy-ion collisions will allow to study the production of light nuclei such as d , t , ${}^3\text{He}$ and their corresponding anti-nuclei. There are two possible production mechanisms for light (anti-)nuclei. The first mechanism is thermal production of nucleus-antinucleus pairs in elementary nucleon-nucleon or parton-parton interactions [7–9]. However, due to their small (\sim few MeV) binding energies, the directly produced nuclei or anti-nuclei are likely to break-up in the medium before escaping. The second mechanism is via final state coalescence of produced (anti-)nucleons or from transported nucleons [10–17]. The quark coalescence as a mechanism of hadron production at intermediate transverse momentum has been well established by studying the number of constituent quark (NCQ) scaling for v_2 of identified hadrons measured at RHIC [18–20, 22–25]. Light nuclei may also be produced via coalescence of quarks similar to the hadrons. But the nuclei formed via quark coalescence is highly unlikely to survive in the high temperature environment due to their small binding energies. In case of hadron formation by quark coalescence, the momentum space distribution of quarks are not directly measurable in experiments. However, in case of nucleon coalescence, momentum space distributions of both the constituents (nucleons) and the products (nuclei) are measurable in heavy-ion collision

experiments. Therefore, measurements of v_2 of light nuclei provides a tool to understand the production mechanism of light nuclei and freeze-out properties at a later stage of the evolution. It also provides an excellent opportunity to understand the mechanism of coalescence at work in high energy heavy-ion collisions.

The production of light (anti-)nuclei has been studied extensively at lower energies in Bevelac at LBNL [26, 27], AGS at RHIC [28, 29] and SPS at CERN [30, 31]. In the AGS experiments, it was found that the coalescence parameter (B_2) is of similar magnitude for both d and \bar{d} indicating similar freeze-out hypersurface of nucleons and anti-nucleons. Furthermore, the dependence of B_2 on collision energy and p_T indicated that light nuclei production is strongly influenced by the source volume and transverse expansion profile of the system [31, 32]. In this paper, we review the results of elliptic flow of light nuclei measured at RHIC and LHC and discuss the possible mechanisms for the light nuclei production.

The paper is organized as follows. Sec. II briefly describes the definition of v_2 , identification of light (anti-)nuclei in the experiments and measurement of v_2 of light (anti-)nuclei. In Sec. III, we present the v_2 results for minimum bias collisions from various experiments. We also discuss the centrality dependence, difference between nuclei and anti-nuclei v_2 as well as the energy dependence of deuteron v_2 . In the same section, we present the atomic mass number scaling and also compare the experimental results with various theoretical models. Finally in Sec. IV, we summarize our observations and discuss the main conclusions of this review.

II. EXPERIMENTAL METHOD

A. Elliptic flow (v_2)

The azimuthal distribution of produced particles in heavy-ion collision can be expressed in terms of a Fourier

* r.haque@uu.nl

† cjena@iisertirupati.ac.in

‡ bedanga@niser.ac.in

TABLE I. Available measurements of light nuclei v_2

Experiment	Nuclei	$\sqrt{s_{NN}}$ (GeV)	Centrality
STAR [38]	$d, \bar{d}, t,$	7.7, 11.5, 19.6, 27,	0-80%, 0-30%, 30-80%
	${}^3\text{He}, {}^3\overline{\text{He}}$	39, 62.4, 200	(0-10%, 10-40%, 40-80% in 200 GeV)
PHENIX [39]	$d+\bar{d}$	200	0-20%, 20-60%
ALICE (Preliminary) [40]	$d+\bar{d}$	2760	0-5%, 5-10%, 10-20%, 20-30%, 30-40%, 40-50%

series,

$$\frac{dN}{d(\phi - \Psi_r)} \propto 1 + \sum_n 2v_n \cos[n(\phi - \Psi_r)], \quad (1)$$

where ϕ is the azimuthal angle of produced particle, Ψ_r is called the reaction plane angle and the Fourier coefficients v_1, v_2 and so on are called flow co-efficients [33]. Ψ_r is defined as the angle between the impact parameter vector and the x-axis of the reference detector in the laboratory frame. Since it is impossible to measure the direction of impact parameter in heavy-ion collisions, a proxy of Ψ_r namely the event plane angle Ψ_n is used for the flow analysis in heavy-ion collisions [34]. The v_2 is measured with respect to the 2^{nd} order event plane angle Ψ_2 [34]. Ψ_2 is calculated using the azimuthal distribution of the produced particles. In an event with N particles, the event plane angle Ψ_2 is defined as [34]:

$$\Psi_2 = \frac{1}{2} \tan^{-1}\left(\frac{Y_2}{X_2}\right). \quad (2)$$

X_2 and Y_2 are defined as

$$X_2 = \sum_{i=1}^N w_i \cos(2\phi_i), \quad (3a)$$

$$Y_2 = \sum_{i=1}^N w_i \sin(2\phi_i), \quad (3b)$$

where w_i are weights given to each particle to optimise the event plane resolution [34, 35]. Usually the magnitude of particle transverse momentum p_T is used as weights as the v_2 increases with p_T . Special techniques are followed while calculating the event plane angle so that it does not contain the particle of interest whose v_2 is to be calculated (self-correlation) and also the non-flow effects (e.g., jets and short range correlations) are removed as much as possible [22, 34, 38]. Heavy-ion experiments use the η -sub event plane method to calculate the elliptic flow of identified hadrons as well as for light nuclei. In this method, each event is divided into two sub-events in two different η -windows (e.g., positive and negative η). Then two sub-event plane angles are calculated with the particles in each sub-event. Each particle with a particular η is then correlated with the sub event plane of the opposite η . This ensures that the particle of interest is not included in the calculation of event plane

angle. A finite η gap is applied between the two sub-events to reduce short range correlations which does not originate from flow.

The distribution of the event plane angles should be isotropic in the laboratory frame for a azimuthally isotropic detector. If the distribution of the event plane angles is not flat in the laboratory frame (due to detector acceptance and/or detector inefficiency) then special techniques are applied to make the distribution uniform. The popular methods to make the Ψ_2 distribution uniform is the ϕ -weight and recentering [36, 37]. In the ϕ -weight method, one takes the actual azimuthal distribution of the produced particle, averaged over large sample of events, and then uses inverse of this distribution as weights while calculating the correlation of the particles with the event plane angle [36, 37]. In the recentering method, one subtracts $\langle X_n \rangle$ and $\langle Y_n \rangle$ from the event-by-event X_n and Y_n , respectively, where $\langle X_n \rangle$ and $\langle Y_n \rangle$ denotes the average of X_n and Y_n over a large sample of similar events. The main disadvantage of applying one of these methods is that it does not remove the contribution from higher flow harmonics. Therefore, another correction method known as the shift correction is used to remove the effects coming from higher flow harmonics. In this method, one fits the Ψ_2 distribution (after applying ϕ -weight and/or recentering method) averaged over all events, with a Fourier function. The Fourier co-efficients from this fit (obtained as fit parameters) are used to shift the Ψ_2 of each event, to make the distribution uniform in the laboratory frame [36, 37].

Since the number of particles produced in heavy-ion collisions are finite, the calculated event plane angle Ψ_2 may not coincide with Ψ_r . For this reason, the measured v_2^{obs} with respect to Ψ_2 is corrected with the event plane resolution factor R_2 , where

$$R_2 = \langle \cos[2(\Psi_2 - \Psi_r)] \rangle. \quad (4)$$

In order to calculate the event plane resolution, one calculates two sub-event plane angles Ψ_2^a and Ψ_2^b , where a and b corresponds to two independent sub-events. If the multiplicities of each sub-event are approximately half of the full event plane, then the resolution of each of sub-event plane can be calculated as [33, 34],

$$\langle \cos[2(\Psi_2^a - \Psi_r)] \rangle = \sqrt{\langle \cos[2(\Psi_2^a - \Psi_2^b)] \rangle}. \quad (5)$$

However, the full event plane resolution can be expressed

as,

$$\begin{aligned} \langle \cos[2(\Psi_2 - \Psi_r)] \rangle &= \frac{\sqrt{\pi}}{2\sqrt{2}} \chi_2 \exp(-\chi_2^2/4) \\ &\times [I_0(\chi_2^2/4) + I_2(\chi_2^2/4)], \end{aligned} \quad (6)$$

where, $\chi_2 = v_2/\sigma$ and I_0, I_2 are modified Bessel functions [33, 34]. The parameter σ is inversely proportional to the square-root of N , the number of particles used to determine the event plane [33, 34]. To calculate the resolution for full event plane (Ψ_2), one has to solve the Eq. (6) iteratively for the value of χ_2 using the subevent plane resolution ($\langle \cos[2(\Psi_2^a - \Psi_r)] \rangle$) which is calculated experimentally using Eq. (5). The χ_2 value is then multiplied with $\sqrt{2}$ as χ_2 is proportional to \sqrt{N} , and re-used in Eq. (6) to calculate the resolution of the full event plane. In a case of very low magnitudes, the full event plane resolution can be approximately given as [33, 34],

$$\begin{aligned} \langle \cos[2(\Psi_2 - \Psi_r)] \rangle &= \sqrt{2} \langle \cos[2(\Psi_2^a - \Psi_r)] \rangle \\ &= \sqrt{2} \langle \cos[2(\Psi_2^a - \Psi_2^b)] \rangle. \end{aligned} \quad (7)$$

The procedure for calculating full and sub-event plane resolutions using sub-event plane angles and various approximations are discussed in detail in [33, 34].

B. Data on light nuclei

For this review, we have collected light nuclei v_2 data from the STAR [38] and PHENIX [39] experiments at RHIC and ALICE experiment at LHC [40]. The table I summarises the measurement of light nuclei v_2 available till date.

C. Extraction of light nuclei v_2

In heavy-ion collisions, light nuclei are primarily identified by comparing the mean ionization energy loss per unit length ($\langle dE/dx \rangle$) in the Time Projection Chamber (TPC) with that from the theoretical predictions ($dE/dx|_{\text{theo}}$) [22, 38, 40–44]. Light nuclei are also identified via the time of flight measurement techniques using the Time-of-Flight (TOF) detector [39, 40, 44–46].

In the STAR experiment, to identify light nuclei using TPC, a variable Z [38] is defined as

$$Z = \log \left[\langle dE/dx \rangle / (dE/dx)|_{\text{theo}} \right]. \quad (8)$$

Then the light nuclei yields are extracted from these Z -distributions in differential p_T and $(\phi - \Psi_2)$ bins for either minimum bias collisions or in selected centrality classes. The $(\phi - \Psi_2)$ distribution is then fitted with a 2^{nd} order Fourier function namely,

$$\frac{dN}{d(\phi - \Psi_2)} \sim 1 + 2v_2 \cos(\phi - \Psi_2). \quad (9)$$

The Fourier co-efficient v_2 is called elliptic flow and is extracted from the fit. As we discussed in the previous subsection this measured v_2 is then corrected with the event plane resolution factor (R_2) [22, 38].

In the ALICE experiment, light nuclei in the low p_T region (< 1.0 GeV/ c for d, \bar{d}) are identified by comparing the variance ($\sigma_{\langle \frac{dE}{dx} \rangle}$) of the measured $\langle dE/dx \rangle$ in the TPC with the corresponding theoretical estimate ($dE/dx|_{\text{theo}}$) [40, 44]. Light nuclei are considered identified if the measured $\langle dE/dx \rangle$ lies within $\pm 3\sigma_{\langle \frac{dE}{dx} \rangle}$ of the $dE/dx|_{\text{theo}}$. On the other hand, the light nuclei yield are extracted from the mass squared (m_{TOF}^2) distribution using the TOF detector. The mass of each particle is calculated using the time-of-flight (t) from the TOF detector and the momentum (\mathbf{p}) information from the TPC [39, 40, 44]. Both the ALICE and PHENIX experiments use the TOF detector to identify light nuclei at high p_T (> 1.0 GeV/ c). The mass of a particle can be calculated using the TOF detector as,

$$m_{\text{TOF}}^2 = \frac{\mathbf{p}^2}{c^2} \left(\frac{c^2 t^2}{L^2} - 1 \right), \quad (10)$$

where the track length L and momentum \mathbf{p} are determined with the tracking detectors placed inside magnetic field [24, 39, 40, 44]. After getting the m^2 for each particle, a selection cut is implemented to reject tracks which have their m^2 several σ away from the true m^2 value of the light nuclei, as done in the STAR experiment [38]. The ALICE experiment, on the other hand defines a quantity Δm such that, $\Delta m = m_{\text{TOF}} - m_{\text{nucl}}$, where m_{nucl} is the mass of the light nuclei under study. The distribution of Δm is then fitted with an Gaussian + exponential function for signal and an exponential function for the background [40]. Then v_2 of light nuclei is calculated by fitting the $v_2(\Delta m)$ with the weighted function,

$$v_2^{\text{Tot}}(\Delta m) = v_2^{\text{Sig}}(\Delta m) \frac{N^{\text{Sig}}}{N^{\text{Tot}}}(\Delta m) + v_2^{\text{Bkg}}(\Delta m) \frac{N^{\text{Bkg}}}{N^{\text{Tot}}}(\Delta m), \quad (11)$$

where the total measured v_2^{Tot} is the weighted sum of that from the signal (v_2^{Sig}) and background (v_2^{Bkg}). The v_2^{Tot} of the candidate particles are calculated using the scalar product method and corrected for the event plane resolution [40].

The PHENIX experiment calculates charged average v_2 of (anti)-deuterons as,

$$v_2 = \langle \cos(2(\phi - \Psi_2)) \rangle / R_2 \quad (12)$$

The quantity $R_2 = \langle \cos(2(\Psi_2 - \Psi_r)) \rangle$ can readily be identified as the resolution of the event plane angle [39]. The resolution of full event plane Ψ_2 is calculated with sub-event planes (Ψ_2^a, Ψ_2^b) estimated using two Beam Beam Counter (BBC) detectors [24, 39]. The detailed procedure of calculating the full event plane resolution from sub-events are already mentioned in the previous subsection. The large η gap between the central TOF and the BBCs ($\Delta\eta > 2.75$) reduces the effects of non-flow significantly [24, 39]. The nuclei v_2 calculated in PHENIX

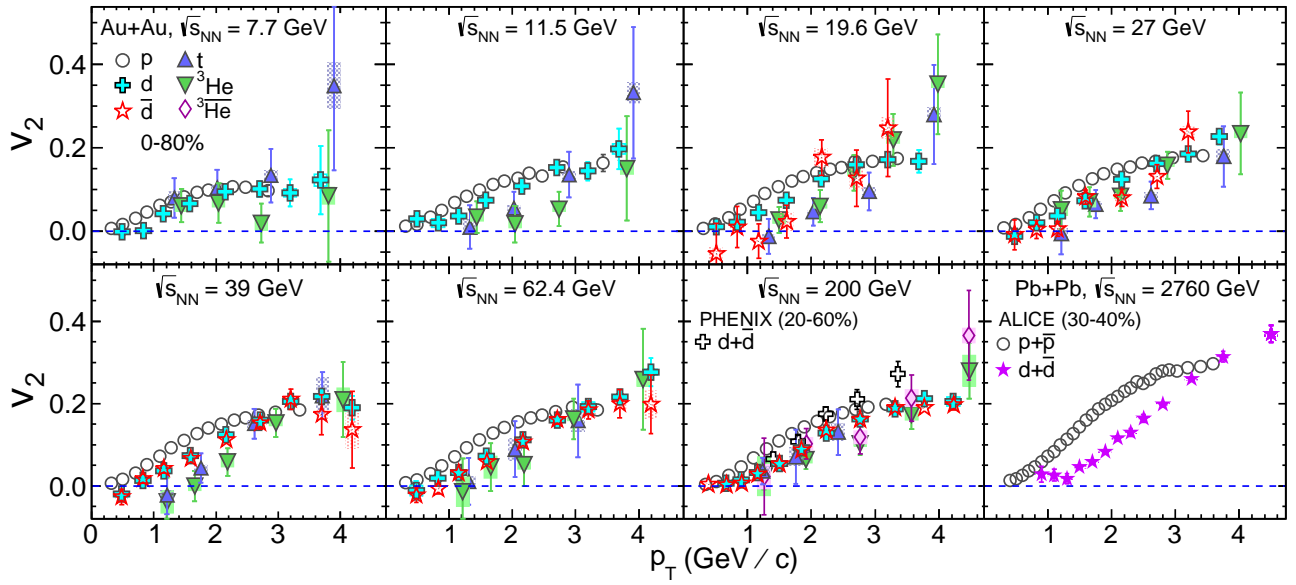


FIG. 1. (color online) Mid-rapidity $v_2(p_T)$ for light nuclei (d , \bar{d} , t , ${}^3\text{He}$, ${}^3\bar{\text{He}}$) in 0-80%, 20-60% and 30-40% centrality from STAR, PHENIX and ALICE, respectively. Proton $v_2(p_T)$ are also shown as open circles [22–24, 47] for comparison. Lines and boxes at each marker corresponds to statistical and systematic errors, respectively.

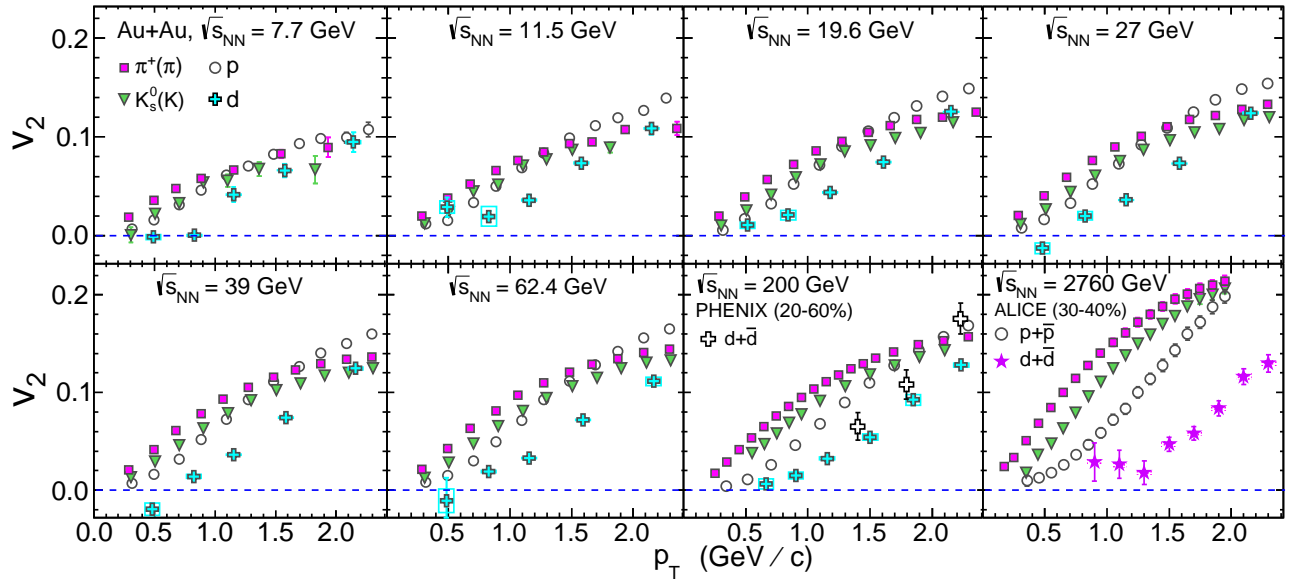


FIG. 2. (color online) Mid-rapidity $v_2(p_T)$ for π^+ (squares), K_s^0 (K in Pb+Pb) (triangles), p (open circles), and d (crosses) in 0-80%, 20-60% and 30-40% centrality from STAR, PHENIX and ALICE, respectively.

is also corrected for the contribution coming from backgrounds, mainly consisting of mis-identification of other particles (*e.g.*, protons) as nuclei. A p_T dependent correction factor was applied on the total v_2 (referred as $v_2^{\text{Sig+Bkg}}(p_T)$) such that,

$$v_2^{d(\bar{d})}(p_T) = [v_2^{\text{Sig+Bkg}}(p_T) - (1 - R)v_2^{\text{Bkg}}(p_T)]/R, \quad (13)$$

where $v_2^{\text{Sig+Bkg}}(p_T)$ is the measured v_2 for $d(\bar{d})$ + background at a given p_T , $v_2^{d(\bar{d})}$ is the corrected v_2 of $d(\bar{d})$ and R is the ratio of Signal and Signal+Background.

III. RESULTS AND DISCUSSION

A. General aspects of light nuclei v_2

Figure 1 shows the energy dependence of light (anti-)nuclei v_2 for $\sqrt{s_{NN}} = 7.7, 11.5, 19.6, 27, 39, 62.4, 200$ and 2760 GeV. The panels are arranged by increasing energy from left to right and top to bottom. The p_T dependence of v_2 of d , \bar{d} , t , ${}^3\text{He}$ and ${}^3\bar{\text{He}}$ is shown for 0-80% centrality in STAR, 20-60% centrality in PHENIX and

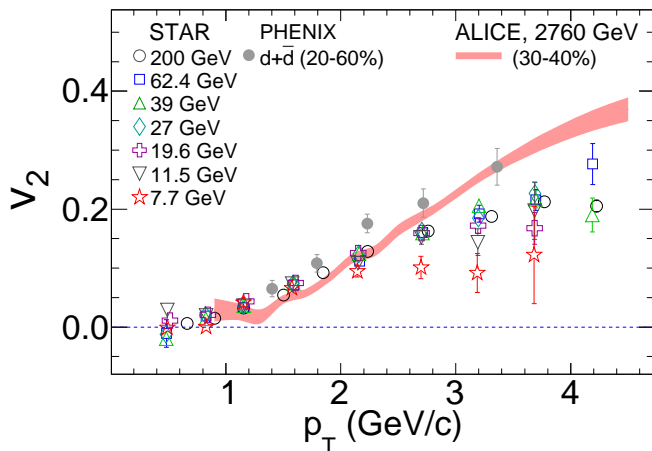


FIG. 3. (color online) Energy dependence of mid-rapidity $v_2(p_T)$ of d for minimum bias (30-40% for ALICE) collisions.

30-40% centrality in ALICE. Since PHENIX and ALICE do not have measurements in the minimum bias collisions, we only show the results for mid-central collisions. The data points of PHENIX and ALICE correspond to inclusive $d+\bar{d}$ v_2 . The general trend of nuclei v_2 of all species is the same— it increases with increasing p_T . The slight difference of v_2 between STAR and PHENIX is due to the difference in centrality ranges. The centrality range for PHENIX is 20-60% and that for STAR is 0-80%.

From the trend in Fig. 1 it seems that light nuclei v_2 shows mass ordering, i.e. heavier particles have smaller v_2 value compared to lighter ones, similar to v_2 of identified particles [22, 24, 47]. In order to see the mass ordering effect more clearly, we restrict the x -axis range to 2.5 GeV/c and compare the v_2 of d with the v_2 of identified particles such as π^+ , K_s^0 (K in Pb+Pb) and p as shown in Fig. 2. We see that d v_2 at all collision energies is lower than the v_2 of the identified hadrons at a fixed value of p_T . Although mass ordering is a theoretical expectation from the hydrodynamical approach to heavy-ion collisions [49], coalescence formalism for light nuclei can also give rise to this effect. Recent studies using AMPT and VISHNU hybrid model suggest that mass ordering is also expected from transport approach to heavy-ion collisions [50, 51]. The v_2 of light nuclei is negative for some collision energies as shown in Fig. 1. This negative v_2 is expected to be the outcome of strong radial flow in heavy-ion collisions [52].

In order to study the energy dependence of light nuclei v_2 , we compare the deuteron v_2 from collision energy $\sqrt{s_{NN}} = 7.7$ GeV to 2760 GeV as shown in Fig. 3. The deuteron $v_2(p_T)$ shows energy dependence prominently for high p_T ($p_T > 2.4$ GeV/c) where v_2 is highest for top collision energy ($\sqrt{s_{NN}} = 2760$ GeV) and gradually decreases with decreasing collision energy. This energy dependent trend of light nuclei v_2 is similar to the energy dependence of identified hadron v_2 where $v_2(p_T)$ also de-

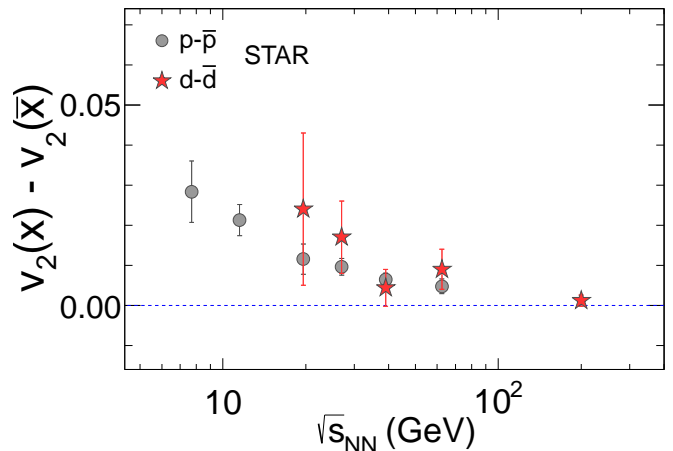


FIG. 4. (color online) Difference of d and \bar{d} $v_2(p_T)$ as a function of collision energy for minimum bias Au+Au collisions in STAR.

creases with decreasing collision energy [22].

The STAR experiment has measured the difference of nuclei (d) and anti-nuclei (\bar{d}) v_2 for collision energies $\sqrt{s_{NN}} = 19.6, 27, 39, 62.4$ and 200 GeV [38]. Figure 4 shows the difference of d and \bar{d} v_2 as a function of collision energy. For comparison, the difference of proton and anti-proton v_2 is also shown [22]. We observe that the difference of d and \bar{d} v_2 remains positive for $\sqrt{s_{NN}} = 7.7 - 39$ GeV. However, for $\sqrt{s_{NN}} \geq 62.4$ GeV the difference of d and \bar{d} v_2 is almost zero. The difference of d and \bar{d} v_2 qualitatively follows the same trend as seen for difference of p and \bar{p} v_2 [22]. It is easy to infer from simple coalescence model that light (anti-)nuclei formed via coalescence of (anti-)nucleons, will also reflect similar difference in v_2 as the constituent nucleon and anti-nucleon. The difference in v_2 between particles and their antiparticles has been attributed to the chiral magnetic effect in finite baryon-density matter [53], different v_2 of produced and transported particles [54], different rapidity distributions for quarks and antiquarks [55], the conservation of baryon number, strangeness, and isospin [56], and different mean-field potentials acting on particles and their antiparticles [57].

The centrality dependence of light nuclei v_2 measured by the STAR and ALICE is shown in Fig. 5. STAR has measured d and \bar{d} v_2 in two different centrality ranges namely 0-30% and 30-80% for collision energies below $\sqrt{s_{NN}} = 200$ GeV. In case of $\sqrt{s_{NN}} = 200$ GeV, the light nuclei v_2 is measured in three different centrality ranges namely 0-10% (central), 10-40% (mid-central) and 40-80% (peripheral) as high statistics data were available. ALICE has measured inclusive $d + \bar{d}$ v_2 in 6 different centrality ranges namely, 0-5%, 5-10%, 10-20%, 20-30%, 30-40% and 40-50%. We only present the results from 0-5%, 20-30% and 40-50% centrality from ALICE as shown in Fig. 5. The v_2 of d shows strong centrality dependence for all collision energies studied in the STAR experiment.

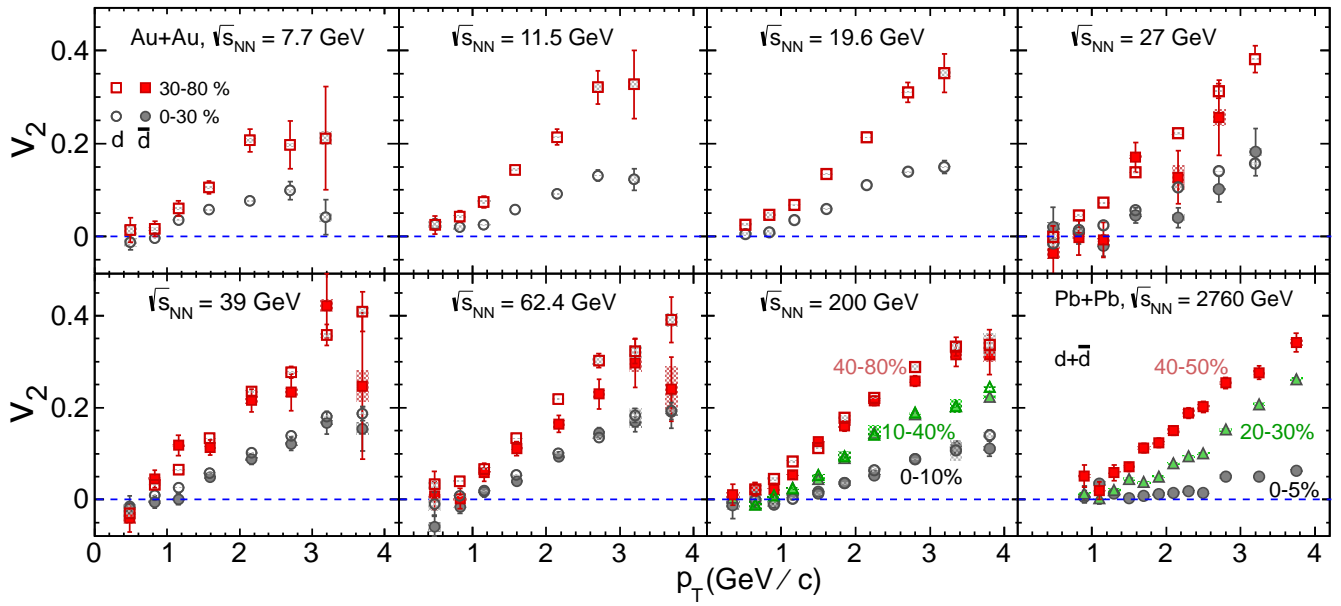


FIG. 5. (color online) Centrality dependence of v_2 of $d(\bar{d})$ as a function of p_T .

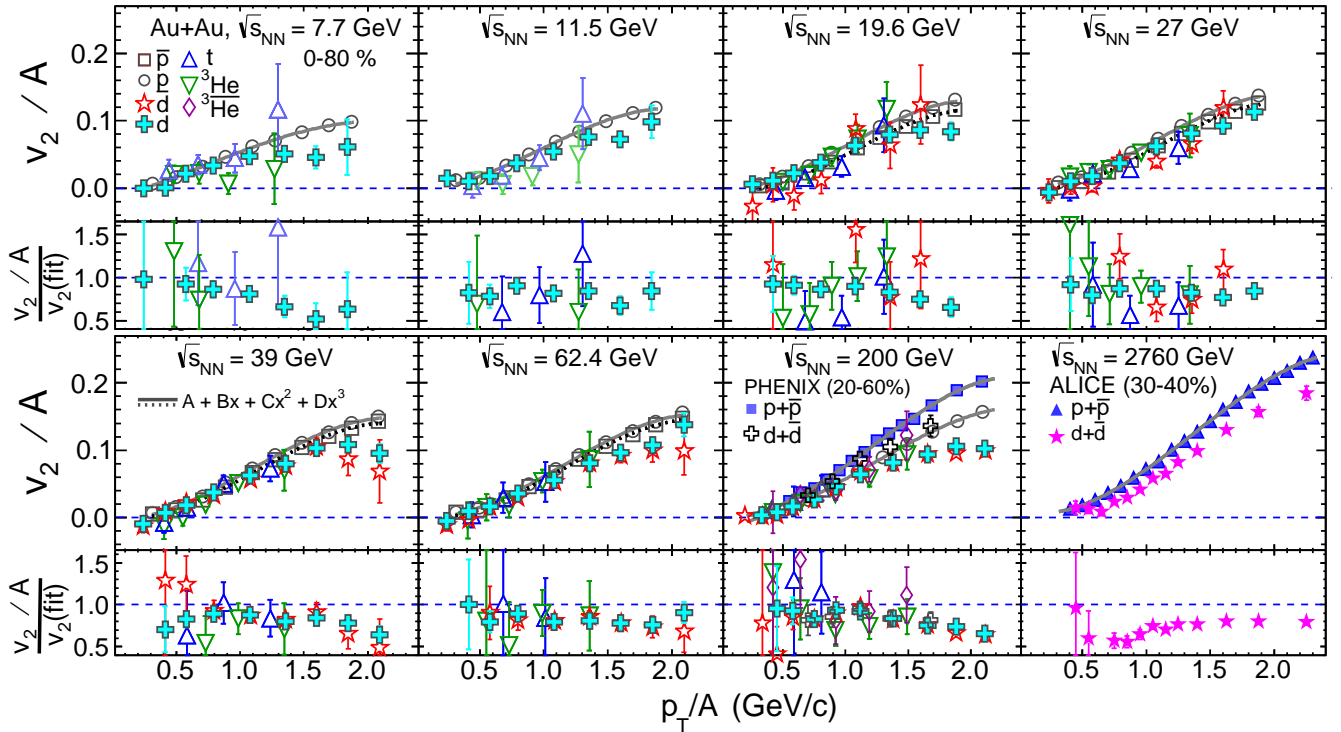


FIG. 6. (color online) Atomic mass number scaling v_2/A of light nuclei as a function of p_T/A for STAR (0-80%), PHENIX (20-60%) and ALICE (30-40%).

We observe that more central events has lower v_2 compared to peripheral events. \bar{d} shows the same trend as d for collision energies down to $\sqrt{s_{NN}} = 27$ GeV. The STAR experiment could not study centrality dependence of \bar{d} below $\sqrt{s_{NN}} = 27$ GeV due to limited event statistics [38]. Comparing the centrality dependence of $d(\bar{d})$ v_2 from STAR and ALICE we can see that both

experiments show strong centrality dependence of light nuclei v_2 . The centrality dependence of light nuclei v_2 is analogous to the centrality dependence observed for identified nucleon (p, \bar{p}) v_2 [58, 59].

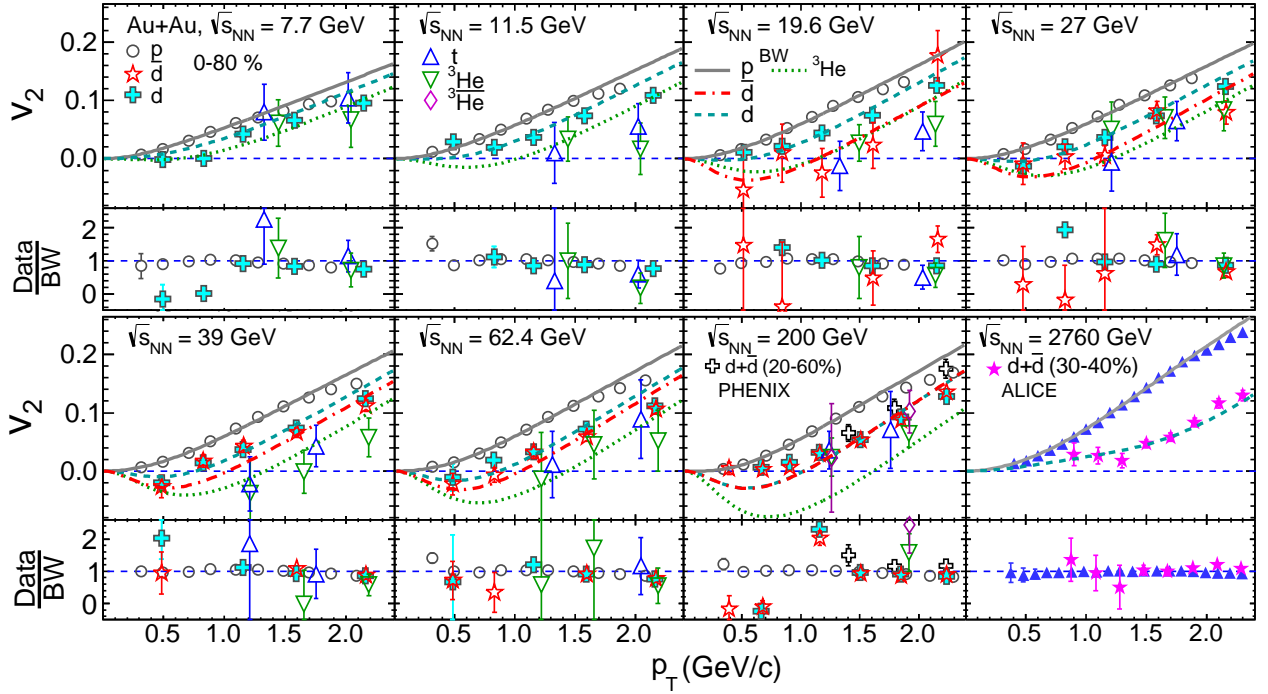


FIG. 7. (color online) Light nuclei v_2 as a function of p_T from blast-wave model (lines). For comparison, $p+\bar{p}$ v_2 is also shown. Marker for STAR corresponds to 0-80%, PHENIX corresponds to 20-60% and ALICE corresponds to 30-40% central events.

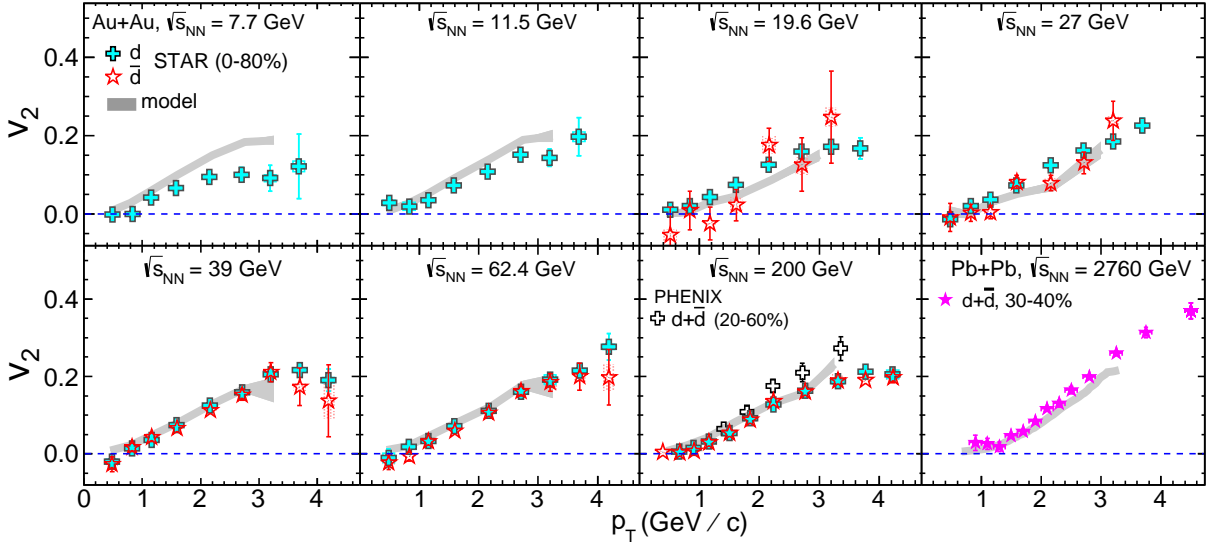


FIG. 8. (color online) Light nuclei v_2 as a function of p_T from AMPT+coalescence model (solid lines). Markers for STAR experiment corresponds to 0-80%, PHENIX corresponds to 20-60% and ALICE corresponds to 30-40% central events.

B. Mass number scaling and model comparison

It is expected from the formulations of coalescence model that if light nuclei are formed via the coalescence of nucleons then the elliptic flow of light nuclei, when divided by atomic mass number (A), should scale with the elliptic flow of nucleons [21]. Therefore, we expect that the light (anti-)nuclei v_2 divided by A , should

scale with $p(\bar{p})$ v_2 . Here, we essentially assume that the v_2 of (anti-)proton and (anti-)neutron are same as expected from the observed NCQ scaling of identified particle v_2 [22]. Figure 6 shows the atomic mass number scaling of light nuclei v_2 from STAR, PHENIX and ALICE experiments. Since ALICE does not have results in minimum bias events, so we used both $p+\bar{p}$ and $d+\bar{d}$ v_2 from 30-40% centrality range. We observe that light nuclei v_2 from STAR and PHENIX show atomic mass

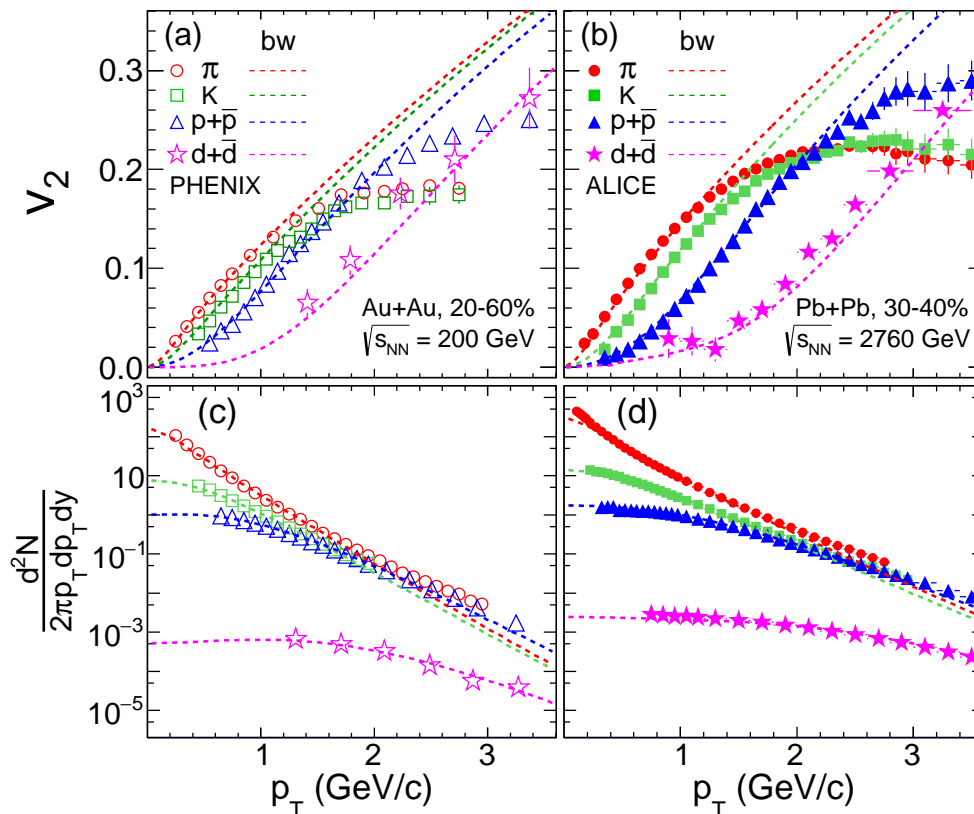


FIG. 9. (color online) (a) Blast-wave fit of π , K , $p(\bar{p})$, $d(\bar{d})$ v_2 and (c) p_T spectra from the PHENIX experiment. Same is shown for the ALICE experiment in the panel (b) and (d). The p_T spectra are used from [25, 64]. Markers for PHENIX data corresponds to 20-60% and markers for ALICE data corresponds to 30-40% central events.

number scaling up to $p_T/A \sim 1.5$ GeV/c. However, deviation of the scaling of the order of 20% is observed for $d+\bar{d}$ v_2 from ALICE. The scaling of light (anti-)nuclei v_2 with (anti-)proton v_2 suggests that light (anti-)nuclei might have formed via coalescence of (anti-)nucleons at a later stage of the evolution at RHIC energies for p_T/A up to 1.5 GeV/c [10–14]. However, this simple picture of coalescence may not be holding for ALICE experiment at LHC energies. On the contrary, there is another method to produce light nuclei, for example by thermal production in which it is assumed that light nuclei are produced thermally like any other primary particles [8, 9]. Various thermal model studies have successfully reproduced the different ratios of produced particles as well as light nuclei in heavy-ion collisions [8, 9].

In order to investigate the success of these models, both STAR and ALICE has compared the elliptic flow of light nuclei with the predictions from blast-wave models [38, 40]. Figure 7 shows the v_2 of light nuclei predicted from blast-wave model using the parameters obtained from fits to the identified particles v_2 [40, 60]. We observe that blast-wave model reproduces v_2 of light nuclei from STAR with moderate success except for low $p_T (< 1.0$ GeV/c) where v_2 of $d(\bar{d})$ are under-predicted for all collision energies. However, the blast-wave model

seems to successfully reproduce the $d+\bar{d}$ v_2 from ALICE. The low relative production of light nuclei compared to identified nucleons at RHIC collisions energies supports the procedure of light nuclei production via coalescence mechanism [10–14]. However, the success of blast-wave model in reproducing the nuclei v_2 at LHC and moderate success at RHIC suggest that the light nuclei production is also supported by thermal process [8, 9]. The light nuclei production in general might be a more complicated coalescence process, *e.g.*, coalescence of nucleons in the local rest frame of the fluid cell. This scenario might give rise to deviations from simple A scaling [38].

At RHIC energies the light nuclei v_2 have been compared with results from a hybrid AMPT+coalescence model [38]. A Multi Phase Transport (AMPT) model is an event generator with Glauber Monte Carlo initial state [61]. The AMPT model includes Zhang’s Partonic Cascade (ZPC) model for initial partonic interactions and A Relativistic Transport (ART) model for later hadronic interactions [61]. The nucleon phase-space information from the AMPT model is fed to the coalescence model to generate light nuclei [38, 62]. Figure 8 shows the light nuclei v_2 from the coalescence model and compared to the data. The coalescence model prediction for $d+\bar{d}$ in Pb+Pb collisions at $\sqrt{s_{NN}} = 2760$ GeV

is taken from [63]. The coalescence model fairly reproduces the measurement from data for all collision energies except for the lowest energy $\sqrt{s_{NN}} = 7.7$ GeV. The AMPT model generates nucleon v_2 from both partonic and hadronic interactions for all the collision energies presented. However, increased hadronic interactions compared to partonic, at lowest collision energies, is not implemented in the AMPT+coalescence model. This could be the reason behind the deviation of the data from the model predictions at lowest collision energy [22].

We have performed simultaneous fit to the v_2 and p_T spectra of identified hadrons + light nuclei using the same blast-wave model as used in [40, 47]. The simultaneous fit of v_2 and p_T spectra for measurements from the PHENIX and the ALICE experiment are shown in Fig. 9. We find that the inclusion of light nuclei results to the fit does not change the fit results compared to the blast-wave fit performed only on identified hadron v_2 and p_T spectra. This indicates that the light nuclei v_2 and p_T spectra is well described by the blast-wave model.

C. Model prediction of ${}^3\text{He}$ and ${}^4\text{He}$ v_2

We have predicted the v_2 of ${}^3\text{He}$ and ${}^4\text{He}$ using the simple coalescence and blast-wave model. Since protons and neutrons have similar masses and same number of constituent quarks, they should exhibit similar collective behavior and hence, similar magnitude of v_2 . Therefore, we parametrize the elliptic flow of $p + \bar{p}$ v_2 using the fit formula [65],

$$f_{v_2(p_T)}(n) = \frac{an}{1 + e^{-(p_T/n-b)/c}} - dn, \quad (14)$$

where a , b , c , and d are fit parameters and n is the constituent quark number of the particle [65]. The fit to $p + \bar{p}$ v_2 (solid lines) from the PHENIX and ALICE experiment is shown in Fig. 10(a) and (b), respectively. Assuming similar magnitude of neutron v_2 as that of proton, we then predict the v_2 of ${}^3\text{He}$ and ${}^4\text{He}$ as,

$$v_2(p_T)_{{}^3\text{He}} \approx 3v_2(p_T/3)_p, \quad (15a)$$

$$v_2(p_T)_{{}^4\text{He}} \approx 4v_2(p_T/4)_p. \quad (15b)$$

This simplified coalescence model prediction of ${}^3\text{He}$ and ${}^4\text{He}$ v_2 are shown in Fig. 10(a) and (b) as blue (thin-dotted) lines. For comparison, the blast-wave model predicted v_2 of ${}^3\text{He}$ and ${}^4\text{He}$ from the fit parameters obtained in Fig. 9 are also shown in red (thick-dotted) lines. We observe characteristic difference is observed in the prediction of ${}^3\text{He}$ and ${}^4\text{He}$ v_2 from the coalescence and the blast-wave model. As one expects from the mass ordering effect of blast-wave model, the v_2 of ${}^3\text{He}$ and ${}^4\text{He}$ almost zero in the intermediate p_T range ($1.0 < p_T < 2.5$ GeV/c). On the other hand, the simple coalescence model predicts orders of magnitude higher v_2 compared to blast-wave for both ${}^3\text{He}$ and ${}^4\text{He}$ in the same p_T range. Hence, experimental measurements of ${}^3\text{He}$ and ${}^4\text{He}$ v_2

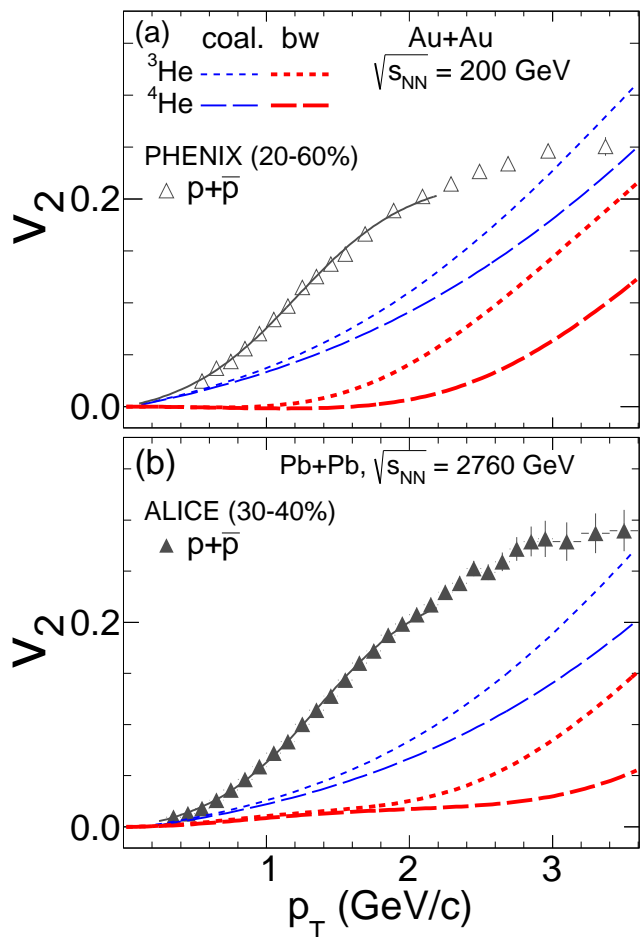


FIG. 10. (color online) (a) Coalescence model predictions (blue lines) of ${}^3\text{He}$ and ${}^4\text{He}$ v_2 for (a) $\sqrt{s_{NN}} = 200$ GeV and (b) for $\sqrt{s_{NN}} = 2760$ GeV. The blast-wave predictions of ${}^3\text{He}$ and ${}^4\text{He}$ v_2 are also shown in red lines.

in future, would significantly improve our knowledge on the mechanisms of light nuclei formation in heavy-ion collisions [44, 66–68].

IV. SUMMARY AND CONCLUSIONS

We have presented a review of elliptic flow v_2 of light nuclei (d , t and ${}^3\text{He}$) and anti-nuclei (\bar{d} and ${}^3\bar{\text{He}}$) from STAR experiment, and inclusive $d + \bar{d}$ v_2 from PHENIX at RHIC and ALICE at LHC. Similar to identified hadrons, the light nuclei v_2 show a monotonic rise with increasing p_T and mass ordering at low p_T for all measured collision energies. The beam energy dependence of d v_2 is small at intermediate p_T and only prominent at high p_T , which is similar to the trend as observed for the charged hadron v_2 . The v_2 of nuclei and anti-nuclei are of similar magnitude for top collision energies at RHIC but at lower collision energies, the difference in v_2 between nuclei and anti-nuclei qualitatively follow the difference in proton and anti-proton v_2 . The centrality

dependence of light (anti-)nuclei $v_2(p_T)$ is similar to that of identified hadrons $v_2(p_T)$.

Light (anti-)nuclei v_2 is found to follow the atomic mass number (A) scaling for almost all collision energies at RHIC suggesting coalescence as the underlying process for the light nuclei production in heavy-ion collisions. However, a deviation from mass number scaling at the level of 20% is observed at LHC. This indicates that a simple coalescence process may not be the only underlying mechanism for light nuclei production. Furthermore, a transport-plus-coalescence model study is found to approximately reproduce the light nuclei v_2 measured at RHIC and LHC. The agreement of coalescence model with the data from PHENIX and STAR are imperceptibly better than the blast-wave model. However, at the LHC energy, the light nuclei v_2 is better described by blast-wave model rather than the simple coalescence model. The coalescence mechanism, intuitively, should be the prominent process of light nuclei production. However, the breaking of mass scaling at LHC energy and success of blast-wave model prevent us to draw any definitive conclusion on the light nuclei production mechanism.

We observed orders of magnitude difference in ${}^3\text{He}$ and ${}^4\text{He}$ v_2 as predicted by blast-wave and coalescence model. The blast-wave model predicts almost zero v_2 for ${}^3\text{He}$ and ${}^4\text{He}$ up to $p_T = 2.5$ GeV/c, whereas the coalescence model predicts significant v_2 for ${}^3\text{He}$ and ${}^4\text{He}$ at same p_T range. Hence, the precise measurements of ${}^3\text{He}$ and ${}^4\text{He}$ v_2 in future can significantly improve the knowledge of the light nuclei production mechanism in heavy-ion collisions.

ACKNOWLEDGEMENTS

We thank STAR collaboration, PHENIX collaboration and ALICE collaboration for providing the light nuclei v_2 data and the model predictions. This work is supported by DAE-BRNS project grant No. 2010/21/15-BRNS/2026 and Dr. C. Jena is supported by XIIth plan project PIC. No. 12-R&D-NIS-5.11-0300. The authors declare that there is no conflict of interest regarding the publication of this paper.

-
- [1] N. Itoh, Prog. Theor. Phys. **44**, 291 (1970); M. A. Stephanov, K. Rajagopal, and E. V. Shuryak, Phys. Rev. Lett. **81**, 4816 (1998); M. A. Stephanov, K. Rajagopal, and E. V. Shuryak, Phys. Rev. D **60**, 114028, (1999); M. A. Stephanov, PoS **LAT2006**, 024 (2006), arXiv:hep-lat/0701002; K. Fukushima and T. Hatsuda, Rep. Prog. Phys. **74**, 014001 (2010).
- [2] I. Arsene *et al.* (BRAHMS collaboration), Nucl. Phys. A **757**, 1 (2005); B. B. Back *et al.* (PHOBOS Collaboration), Nucl. Phys. A **757**, 28 (2005); J. Adams *et al.* (STAR Collaboration), Nucl. Phys. A **757**, 102 (2005); K. Adcox *et al.* (PHENIX Collaboration), Nucl. Phys. A **757**, 184 (2005).
- [3] S. Gupta, X. Luo, B. Mohanty, H. G. Ritter, N. Xu, Science **332**, 1525 (2011).
- [4] L. Adamczyk *et al.* (STAR Collaboration), Phys. Rev. Lett. **112**, 032302 (2014).
- [5] K. Aamodt *et al.* (ALICE Collaboration), J. Instrum. **3**, S08002 (2008); B.B. Abelev *et al.* (ALICE Collaboration), Int. J. Mod. Phys. A **29**, 1430044 (2014).
- [6] G. Lemaître, Annales de la société Scientifique de Bruxelles **47**, 49 (1927).
- [7] A. Mekjian, Phys.Rev. C **17**, 1051 (1978); P. Siemens and J. I. Kapusta, Phys.Rev.Lett. **43**, 1486 (1979).
- [8] P. Braun-Munzinger and J. Stachel, J. Phys. G **21**, L17 (1995); P. Braun-Munzinger and J. Stachel, J. Phys. G **28**, 1971 (2002); A. Andronic, P. Braun-Munzinger, J. Stachel and H. Stöcker, Phys. Lett. B **697**, 203 (2011); J. Stachel, A. Andronic, P. Braun-Munzinger and K. Redlich, J. Phy. Conf. **509**, 01201 (2014).
- [9] S. Chatterjee and B. Mohanty, Phys. Rev. C **90**, 034908 (2014).
- [10] S. T. Butler and C. A. Pearson, Phys. Rev. **129**, 836 (1963); A. Schwarzschild and C. Zupancic, Phys. Rev. **129**, 854 (1963).
- [11] H. H. Gutbrod *et al.*, Phys. Rev. Lett. **37**, 667 (1976).
- [12] H. Sato and K. Yazaki, Phys. Lett. B **98**, 153 (1981); E. Remler, Annals Phys. **136**, 293 (1981); M. Gyulassy, K. Frankel, and E. Remler, Nucl. Phys. A **402**, 596 (1983). L. Csernai and J. I. Kapusta, Phys. Rept. **131**, 223 (1986).
- [13] P. Danielewicz and G. Bertsch, Nucl. Phys. A **533**, 712 (1991); C. B. Dover, U. W. Heinz, E. Schnedermann, and J. Zimanyi, Phys. Rev. C **44**, 1636 (1991).
- [14] W. J. Llope *et al.*, Phys. Rev. C **52**, 2004 (1995); J. Nagle, B. Kumar, D. Kusnezov, H. Sorge, and R. Mattiello, Phys. Rev. C **53**, 367 (1996).
- [15] R. Scheibl and U. Heinz, Phys. Rev. C **59**, 1585 (1999).
- [16] S. Zhang, J. Chen, H. Crawford, D. Keane, Y. Ma, *et al.*, Phys. Lett. B **684**, 224 (2010); J. Steinheimer, K. Gudima, A. Botvina, I. Mishustin, M. Bleicher, *et al.*, Phys.Lett. B **714**, 85 (2012).
- [17] St. Mrówczyński, Acta Physica Polonica B **48**, 707 (2017).
- [18] S. A. Voloshin, Nucl. Phys. A **715**, 379 (2003).
- [19] D. Molnar and S.A. Voloshin, Phys. Rev. Lett. **91**, 092301 (2003).
- [20] R. C. Hwa and C. B. Yang, Phys. Rev. C **67**, 064902 (2003); R. J. Fries, B. Muller, C. Nonaka, and S. A. Bass, Phys. Rev. Lett. **90**, 202303 (2003).
- [21] T. Z. Yan, Y. G. Ma, X. Z. Cai *et al.*, Phys. Lett. B **638**, 50 (2006); Y. Oh and C. M. Ko, Phys. Rev. C **76**, 054910 (2007).
- [22] L. Adamczyk *et al.* (STAR Collaboration), Phys. Rev. C **88**, 014902 (2013); L. Adamczyk *et al.* (STAR Collaboration), Phys. Rev. Lett. **110**, 142301 (2013).
- [23] L. Adamczyk *et al.* (STAR Collaboration), Phys. Rev. Lett. **116**, 062301 (2016).

- [24] S. S. Adler *et al.* (PHENIX Collaboration), Phys. Rev. Lett. **91**, 182301 (2003).
- [25] S. S. Adler *et al.* (PHENIX Collaboration), Phys. Rev. C **69**, 034909 (2004).
- [26] S. Nagamiya *et al.*, Phys. Rev. C **24**, 971 (1981); H. H. Gutbrod *et al.*, Phys. Rev. Lett. **37**, 667 (1976); R. L. Auble *et al.*, Phys. Rev. C **28**, 1552 (1983).
- [27] S. Wang *et al.*, (EOS Collaboration), Phys. Rev. Lett. **74**, 2646 (1995); M. A. Lisa *et al.*, (EOS Collaboration), Phys. Rev. Lett. **75**, 2662 (1995).
- [28] M. Aoki *et al.*, Phys. Rev. Lett. **69**, 2345 (1992).
- [29] T. A. Armstrong *et al.* (E864 Collaboration), Phys. Rev. Lett. **85**, 2685 (2000); J. Barrette *et al.* (E877 Collaboration), Phys. Rev. C **61**, 044906 (2000); S. Albergo *et al.*, Phys. Rev. C **65**, 034907 (2002).
- [30] S. Kabana (for the NA52 collaboration) Nucl. Phys. A **638**, 411c (1998); T. Anticic *et al.* (NA49 Collaboration), Phys. Rev. C **85**, 044913 (2012); G. Melkumov (for the NA49 collaboration), PoS CPOD07, 024 (2007); V. I. Kolesnikov (for the NA49 Collaboration), J. Phys. Conf. Ser. **110**, 032010 (2008).
- [31] I. G. Bearden *et al.*, Phys. Rev. Lett. **85**, 2681 (2000).
- [32] A. Polleri *et al.*, Phys. Lett. B **419**, 19 (1998).
- [33] S. Voloshin and Y. Zhang, Z Phys C **70**, 665 (1996).
- [34] A. M. Poskanzer and S. A. Voloshin, Phys. Rev. C **58**, 1671 (1998).
- [35] P. Danielewicz, Phys. Rev. C **51**, 716 (1995).
- [36] E877 Collaboration, J. Barrette *et al.*, Phys. Rev. C **56**, 3254 (1997).
- [37] E877 Collaboration, J. Barrette *et al.*, Phys. Rev. C **55**, 1420 (1997).
- [38] L. Adamczyk *et al.* (STAR Collaboration), Phys. Rev. C **94**, 034908 (2016).
- [39] S. Afanasiev *et al.* (PHENIX Collaboration), Phys. Rev. Lett. **99**, 052301 (2007).
- [40] S. Acharya *et al.* (ALICE Collaboration), arXiv:1707.07304 [nucl-ex].
- [41] M. Anderson *et al.* (STAR Collaboration), Nucl. Instrum. Methods A **499**, 659 (2003).
- [42] J. Adams *et al.* (STAR Collaboration), Physics Letters B **637** 161 (2006).
- [43] J. Alme *et al.*, Nucl. Instrum. Meth. A **622**, 316 (2010).
- [44] J. Adam *et al.* (ALICE Collaboration), Phys. Rev. C **93**, 024917 (2016).
- [45] W. J. Llope, Nucl. Instrum. Methods B **241**, 306 (2005); W. J. Llope, Nucl. Instrum. Methods A **661**, S110 (2012).
- [46] A. Akindinov *et al.*, Eur. Phys. J. Plus **128**, 44 (2013).
- [47] Francesco Noferini (for the ALICE Collaboration), JHEP **06**, 190 (2015).
- [48] S. A. Voloshin, A. M. Poskanzer and R. Snellings, in Landolt-Boernstein, Relativistic Heavy Ion Physics, Vol. 1/23, p 5-54 (Springer-Verlag,2010); arXiv:0809.2949 [nucl-ex].
- [49] P. Huovinen, P. F. Kolb, U. W. Heinz, P. V. Ruuskanen, and S. A. Voloshin, Phys. Lett. B **503**, 58 (2001).
- [50] H. Li *et al.*, Phys. Rev. C **93**, 051901 (2016), H. Li *et al.*, arXiv:1604.07387.
- [51] H. Xu, Z. Li, H. Song, Phys. Rev. C **93**, 064905 (2016).
- [52] S. A. Voloshin, A. M. Poskanzer and R. Snellings, Landolt-Börnstein series, Springer-Verlag, Berlin Germany, Vol. 23, p. 293 (2010), arXiv:0809.2949v2 [nucl-ex].
- [53] Y. Burnier, D. E. Kharzeev, J. Liao, and H.U. Yee, Phys. Rev. Lett **107**, 052303 (2011).
- [54] J. C. Dunlop, M. A. Lisa, and P. Sorensen, Phys. Rev. C **84**, 044914 (2011).
- [55] V. Greco, M. Mitrovski, and G. Torrieri, Phys. Rev. C **86**, 044905 (2012).
- [56] J. Steinheimer, V. Koch, and M. Bleicher Phys. Rev. C **86**, 044903 (2012).
- [57] J. Xu, L. W. Chen, C. M. Ko and Z. W. Lin, Phys. Rev. C **85**, 041901(R) (2012); J. Xu, T. Song, C. M. Ko, and F. Li, Phys. Rev. Lett. **112**, 012301 (2014); T. Song, S. Plumari, V. Greco, C. M. Ko, F. Li, arXiv:1211.5511 [nucl-th]; J. Xu, C.M. Ko, F. Li, T. Song, and H. Liu, arXiv:1407.3882v3 [nucl-th].
- [58] L. Adamczyk *et al.* (STAR Collaboration), Phys. Rev. C **93**, 014907 (2016).
- [59] B. Abelev *et al.* (ALICE Collaboration), JHEP **06**, 190 (2015).
- [60] X. Sun, H. Masui, A. M. Poskanzer, and A. Schmah, Phys. Rev. C **91**, 024903 (2015).
- [61] Z. Lin, C. M. Ko, B. A. Li, B. Zhang, and S. Pal, Phys. Rev. C **72**, 064901 (2005).
- [62] M. R. Haque, Ph.D Thesis, NISER India, <https://drupal.star.bnl.gov/STAR/theses/phd-67>
- [63] Lilin Zhu, Che Ming Ko, and Xuejiao Yin Phys. Rev. C **92**, 064911 (2015).
- [64] B. Abelev *et al.* (ALICE Collaboration), Phys. Lett. B **736**, 196 (2014).
- [65] X. Dong, S. Esumi, P. Sorensen, N. Xu, and Z. Xu, Phys. Lett. B **597**, 328 (2004).
- [66] H. Agakishiev *et al.* (STAR Collaboration), Nature **473**, 353 (2011).
- [67] B. I. Abelev *et al.* (STAR Collaboration), Science **328**, 58 (2010).
- [68] J. Adam *et al.* (ALICE Collaboration), Physics Letters B **754**, 360 (2016).